



Provided by the author(s) and University of Galway in accordance with publisher policies. Please cite the published version when available.

Title	Determination of flushing characteristics of the Irish Sea: A spatial approach
Author(s)	Dabrowski, Tomasz; Hartnett, Michael T.; Olbert, Agnieszka Indiana
Publication Date	2011-12-08
Publication Information	Dabrowski, T,Hartnett, M,Olbert, AI (2012) 'Determination of flushing characteristics of the Irish Sea: A spatial approach'. Computers & Geosciences, 45 :250-260.
Publisher	Elsevier ScienceDirect
Link to publisher's version	<a href="http://dx.doi.org/10.1016/j.cageo.2011.11.023">http://dx.doi.org/10.1016/j.cageo.2011.11.023</a>
Item record	<a href="http://hdl.handle.net/10379/5842">http://hdl.handle.net/10379/5842</a>
DOI	<a href="http://dx.doi.org/10.1016/j.cageo.2011.11.023">http://dx.doi.org/10.1016/j.cageo.2011.11.023</a>

Downloaded 2024-04-17T21:31:45Z

Some rights reserved. For more information, please see the item record link above.



1 **Determination of flushing characteristics of the Irish Sea: a**  
2 **spatial approach**  
3

4 Tomasz Dabrowski, Michael Hartnett, Agnieszka I. Olbert

5 *Civil Engineering Department / Ryan Institute for Environmental, Marine and Energy*  
6 *Research, National University of Ireland, Galway.*

7  
8

9 **Abstract**

10 The Authors devised a novel generic approach to assessing the flushing of the Irish  
11 Sea through the determination of spatially distributed residence times and the  
12 development of flushing homogeneity curves. Results indicate that flushing of the  
13 Irish Sea is both spatially and temporally highly variable. Average residence times  
14 of the material introduced in winter may be up to 28% higher than the material  
15 introduced in summer, and the aerial flushing deviation index may reach up to 470  
16 days. The spatial approach to flushing is an extremely useful complement to  
17 classical flushing analysis considering significant implications for management of  
18 water quality.

19

20 **Keywords:** numerical modelling, Irish Sea, residence time, flushing, shelf seas,  
21 thermohaline circulation

22

23

24 **1. Introduction**

25 Coastal waters remain under great threat from many aspects of human activity.  
26 [Cohen et al. \(1997\)](#) estimate that about 50% of global population lives within the  
27 coastal zone; much of the waste generated by these communities end in coastal  
28 waters. Local hydrodynamic regimes of coastal waters are responsible for such

29 important issues as the distribution of effluents, transport of oil spills, sediments and  
30 other materials. Many natural chemical, physical and biological processes occurring  
31 within particular environments, including such important factors as low oxygen  
32 levels or eutrophication, are influenced by circulation patterns. The knowledge of  
33 hydrodynamic regimes in coastal waterbodies, being it ports and marinas, estuaries,  
34 bays and larger coastal embayments, shelf seas, but also ocean basins, is therefore  
35 desirable for engineers, scientists, managers and by policy makers.

36 An important physical attribute of each waterbody is the time scale characteristic  
37 that describes its ability to renew water contained in it. In literature, it is most often  
38 referred to as the flushing or residence time, (e.g. Bolin and Rodhe, 1973;  
39 Zimmerman, 1976; Takeoka, 1984; Dyer, 1997; Luketina, 1998). Water circulation  
40 in a given waterbody is a resultant of various forces, such as tide, wind and density  
41 structure; knowledge of water renewal times can significantly aid the assessment of  
42 the environmental state of waterbodies and their sustainable management.

43 The Irish Sea is a semi-enclosed shelf sea located between the islands of Ireland and  
44 Great Britain, see Figure 1. Water circulation and associated water quality issues  
45 concerning the Irish Sea have drawn the attention of more than a few researchers  
46 over the past few decades (Ramster and Hill, 1969; Simpson and Hunter, 1974;  
47 Proctor, 1981; Jefferies et al., 1982; Prandle, 1984; McKay and Baxter, 1985;  
48 McKay and Pattenden, 1993; Hill et al., 1997; Horsburgh et al., 2000; Dabrowski  
49 and Hartnett, 2008; Wang et al., 2008; Dabrowski et al., 2010). Being an area of  
50 important fishery activities (Hill et al., 1996) and simultaneously exposed to effluent  
51 discharges from multiple estuarine systems located on the Irish and British coasts as  
52 well as from offshore outfalls and subject to further development of the marine  
53 renewable energy sector, it is important that flow patterns and residence times  
54 within the Irish Sea are well understood.

55 Hydrographically, the Irish Sea, located between 52-55N and 3-6W, is a complex  
56 system where two tidal waves interact, and where wind and density-driven  
57 circulations also play an important role. Flushing and transport of pollutants are not  
58 well understood in the region. Previous efforts directed at estimation of the Irish Sea  
59 residence times did not include the complexity of circulation (Jefferies et al., 1982;  
60 Prandle, 1984; McKay and Baxter, 1985; McKay and Pattenden, 1993). Due to large  
61 variations in the published values of residence times, the authors concluded that the  
62 approach taking into account spatial variability of residence times is necessary.  
63 For a more detailed description of the oceanography of the Irish Sea the reader is  
64 referred to Bowden (1980).

65 In this paper, the objectives were to determine water renewal time scales in the Irish  
66 Sea and to analyze complex flushing in the region. The methodology used by the  
67 authors involves calculations of spatially distributed residence times and  
68 development of the flushing homogeneity curves (FHC); the approach is based on  
69 the application of a three-dimensional general ocean and coastal circulation and  
70 transport model. This model was applied previously to the region to investigate  
71 residence times in the eastern Irish Sea as well as travel times from the Sellafield's  
72 nuclear plant outfall site to various regions of the Irish Sea giving good agreement  
73 with previously reported estimates ([Dabrowski and Hartnett, 2008](#)). The model was  
74 also applied to examine the influence of the western Irish Sea gyre developing in  
75 spring and summer on net flows, turn-over and residence times in the region  
76 ([Dabrowski et al., 2010](#)). In this paper, the authors examine the complete Irish Sea  
77 and also its three hydrographically diverse subregions, therefore the analysis of  
78 spatial detail in residence times and development of FHC are required. The  
79 advantage of using a numerical model for the purpose of the flushing properties  
80 analysis is that it gives an additional insight into the impact of various physical

81 processes upon the derived water renewal time scale characteristic. Impacts can be  
82 analyzed by excluding and including various forcing functions in the model.  
83 The layout of the paper is as follows. Section 2 describes the methodology and  
84 model setup, Section 3 provides a brief model calibration report followed by the  
85 presentation and discussion of the results from the flushing simulations in Section 4,  
86 before drawing final conclusions in Section 5.

87

## 88 **2. Method**

### 89 **2.1. Model description**

90 In this study, a three-dimensional numerical model, ECOMSED, was applied to  
91 investigate water renewal time scales in the Irish Sea; the model is described in  
92 detail in [Blumberg and Mellor \(1987\)](#). Below, the main features of the model and  
93 details of its application to the Irish Sea are presented.

94 The bathymetry data of the Irish Sea was interpolated onto a 2 km rectangular finite  
95 difference grid developed for the purpose of this study. The model domain is  
96 delineated in Figure 1. Observations show that the density field in the Irish Sea is  
97 controlled primarily by temperature from early summer onwards (Horsburgh, 1999).  
98 For this reason, and due to the uncertainty in the salinity of inflowing oceanic water,  
99 salinity was held constant at the open boundaries and set to climatologies. Tides  
100 were imposed at the open sea boundaries as tidal constituents and the amplitudes  
101 and phases of  $M_2$ ,  $S_2$ ,  $N_2$ ,  $K_1$ ,  $P_1$  and  $O_1$  constituents were provided. Freshwater  
102 inputs along the British and Irish Coasts were included in the model and distributed  
103 according to values provided in ISSG (1991). Sea temperatures at the open ocean  
104 boundaries were specified at every computational time step, and the values were  
105 obtained by a linear interpolation of monthly data from Meteorological Service  
106 (1995) between the dates. A series of runs were performed to find an optimal surface

107 heat flux model among those incorporated within ECOMSED, as well as appropriate  
108 parameter settings.

109 The bathymetry map is presented in Figure 1 along with the distribution of locations  
110 where tidal elevations (T1-T14) and tidal currents (C1-C14) were available for the  
111 model validation.

112 A full set of meteorological conditions was collated in order to perform seasonal  
113 simulations. The calendar year of 1995 was chosen for simulations, which was  
114 determined by data availability, and the fact that the existence of a well-established  
115 western Irish Sea gyre in that year was already reported (Horsburgh, 1999).

116 Rationale for selecting this year for studying flushing properties of the Irish Sea is  
117 discussed in more details in [Dabrowski et al. \(2010\)](#). Forcing data was obtained  
118 from the US National Oceanic and Atmospheric Administration. This data originates  
119 from the reanalysis/forecast system performing data assimilation using past data  
120 from 1948 to the present.

121 The model solves the advection-diffusion equation to predict spatial distribution of  
122 active (temperature and salinity) and passive tracers; MPDATA advection algorithm  
123 developed by [Smolarkiewicz \(1984\)](#) has been applied. Horizontal diffusion is  
124 calculated according to the formula developed by [Smagorinsky \(1963\)](#), which  
125 adjusts the scale of mixing to the grid size. Horizontal Prandtl number, being the  
126 ratio of horizontal viscosity to horizontal diffusivity, was held constant and set equal  
127 to the recommended value of 1.0 (Hydroqual, 2002). The value of the Smagorinsky  
128 coefficient was fixed at 0.1 as suggested by [Mellor \(2003\)](#). Small-scale mixing not  
129 directly resolved by the model is parameterized in terms of horizontal mixing  
130 coefficients. Turbulence closure scheme is based on the 2.5 level algebraic stress  
131 equations developed by [Mellor and Yamada \(1982\)](#) with recent corrections  
132 presented in [Mellor \(2001\)](#). Vertical Prandtl number, being the ratio of vertical

133 viscosity to vertical diffusivity, and the background mixing parameter were set equal  
134 to the recommended values of 1.0 and  $10^{-6}$  m<sup>2</sup>/s (Hydroqual, 2002), respectively.  
135 The above settings proved to be successful in the reconstruction of the distribution  
136 of Tc-99 (Olbert et al., 2010a, 2010b) and water temperatures in the Irish Sea  
137 ([Dabrowski et al., 2010](#); [Olbert et al., 2011](#)).  
138 Further details on collated data can be found in [Dabrowski \(2005\)](#).

139

## 140 **2.2. Water renewal time scale calculations**

141 A concept of residence time derived in [Takeoka \(1984\)](#) was utilised in this study as  
142 being the most suitable characteristic for describing exchange processes, when the  
143 total material in a reservoir is considered. [Takeoka \(1984\)](#) introduced the remnant  
144 function,  $r(t)$ , as the ratio of the mass of material within a reservoir at a given time to  
145 the initial mass of this material, and defined the average residence time,  $\tau_r$ , as  
146 follows:

$$147 \quad \tau_r = \int_0^{\infty} r(t) dt \quad (1)$$

148 Amongst the researchers who have utilised the above definition of the average  
149 residence time was [Murakami \(1991\)](#), who developed a universal formula for the  
150 remnant function, capable of representing the dye decay curves for basically any  
151 reservoir with the tidal exchange:

$$152 \quad r(t) = \exp(-A_1 t^{B_1}) = \frac{c(t)}{c_0} \quad (2)$$

153 The empirical constants  $A_1$  and  $B_1$  depend on the shape of the decay curve and must  
154 be determined for each case. An additional advantage of [Murakami's](#) expression is  
155 the fact that it can be easily integrated numerically giving the value of the residence  
156 time of a studied reservoir.

157 It can be easily shown that under the assumption of complete mixing, the residence  
158 time of a reservoir equals the time required to reduce the initial concentration of a  
159 tracer by an exponential factor  $e$ , see for example van de Kreeke (1983) and Asselin  
160 and [Spaulding \(1993\)](#). In this study, we treat individual numerical model's cells as  
161 completely mixed reactors, therefore we calculate the e-folding time,  $\tau_e$ , of each cell  
162 to compute the spatial distribution of residence time.

163

### 164 **2.3. Summary of methodology**

165 The three-dimensional ocean and coastal circulation and transport model was  
166 applied to develop a barotropic and baroclinic model of the Irish Sea. Following its  
167 calibration, passive tracer simulations were carried out to track spatial and temporal  
168 distribution of the conservative tracer following its initial uniform distribution  
169 throughout four regions presented in Figure 2. The tracer was introduced in the  
170 model in the form of an instantaneous release and was uniformly dispersed  
171 throughout the regions of interest. Four selected regions are distinct with regards to  
172 the topographical features as well as the circulation patterns. Region A consists of  
173 the entire Irish Sea. Region B is northern Irish Sea; this is a region of enhanced  
174 fishery activity and its western section is subject to strong thermal stratification.  
175 Region C covers the area of the St. George's Channel only. It is the region of highly  
176 energetic tidal circulation; it is vertically well mixed and is also bounded by strong  
177 baroclinic features developing seasonally. Region D, the eastern Irish Sea, is  
178 separated from the main channel running south-north; it is considerably shallower  
179 and receives high input of contaminants from several major estuaries.

180 Dye decay curves,  $c(t)/c_0 = f(t)$ , obtained from the simulations were approximated  
181 by the remnant function,  $r(t)$ , equation (2), using the least squares method.  
182 Integration of  $r(t)$ , equation (1), yields the average residence times of the examined



183 regions. Calculated average residence times are representative of the entire regions,  
184 i.e. tracer concentrations were averaged horizontally and vertically. Influence of  
185 thermal stratification and associated baroclinic features developing in the Irish Sea,  
186 such as the western Irish Sea gyre, which affects water exchange processes in the  
187 region, has been a subject of a separate research presented in Dabrowski et al.  
188 (2010).

189 Five flushing simulations for each region were carried out in this study; the  
190 simulations differed in the tracer release date and forcing functions applied. Two  
191 release dates were considered, summer (1<sup>st</sup> of June, runs F1 – F4) and winter (1<sup>st</sup> of  
192 December, run F5), and four versions of the model comprised following forcing  
193 functions: tides only (run F1), tides and wind stress (run F2), tides and heat fluxes  
194 (run F3), tides, wind stress and heat fluxes (runs F4 and F5). A characterisation of  
195 the simulations is presented in Table 1.

196 Finally, the  $e$ -folding times for each computational cell were computed and  
197 presented as contour plots, showing the distribution of residence time with flushing  
198 pathways clearly marked. On the basis of the spatial distribution of residence time,  
199 FHC were developed summarising percentage area distribution of residence times  
200 throughout the regions. The authors also proposed the aerial flushing deviation  
201 index, FDI, as a useful measure of the spread in the values of distributed residence  
202 times. FDI is the difference between the values of  $\tau_e$ ,  $\tau_{e90\%}$  and  $\tau_{e10\%}$ , for which 10%  
203 of the area are characterised by greater and lower distributed residence times,  
204 respectively. Therefore, FDI also represents the average slope of FHC.

205

### 206 **3. Model Validation**

207 The general tidal circulation in the Irish Sea predicted by the model follows the  
208 pattern described in the literature ([Bowden, 1980](#); [ISSG, 1991](#)). Contours of the

209 model-predicted depth-averaged tidal currents on a spring tide are presented in  
210 Figure 3(a). The model reflects all features of the tidal circulation within the region  
211 properly, for example strong currents in St. George's and North Channels as well as  
212 the area of persistent slack water to the east of the Isle of Man. The extents of the  
213 regions of fast flow, exceeding 1.2 m/s, in the St. George's, the North and the Bristol  
214 Channels as well as the slack water in the Western Irish Sea are in close agreement  
215 with the observations; see ISSG (1991). Magnification of tidal currents near  
216 headlands was observed, as predicted by previous models (Horsburgh, 1999;  
217 Proctor, 1981). An important feature from the point of view of this research work is  
218 the model's ability to predict locations of thermal fronts, with particular emphasis  
219 placed on the western Irish Sea region, which stratifies during late spring and  
220 summer each year. [Simpson and Hunter \(1974\)](#) proposed that the spatial pattern of  
221 seasonal stratification is controlled by the distribution of tidal mixing as summarized  
222 by the parameter  $H/v_s^3$ , where  $H$  is the water depth, and  $v_s$  is the maximum tidal  
223 surface current. Figure 3(b) presents the spatial distribution of the  $\log[H/v_s^3]$   
224 parameter predicted by the model; contours of  $\log[H/v_s^3] = 2$ , which according to  
225 [Simpson et al. \(1977\)](#) determine the locations of thermal fronts, are labelled. The  
226 spatial distribution of this parameter predicted by our model corresponds closely to  
227 that observed by [Simpson et al. \(1977\)](#) in: the western Irish Sea, the southern  
228 reaches of the St. George's Channel as well as in Cardigan Bay to the east of the St.  
229 George's Channel. Comparisons of model-predicted and recorded tidal elevations at  
230 selected coastal location (T14) and predicted and recorded currents over a tidal cycle  
231 at location B3 in the western Irish Sea are also presented in Figure 3(c) and 3(d),  
232 respectively. As can be seen, very good agreement with the observations has been  
233 achieved for the barotropic component of the hydrodynamic model. The presented

234 comparisons are typical of the good correlation obtained between model predictions  
235 and data for many locations throughout the Irish Sea.

236 Application of the heat flux model by [Ahsan and Blumberg \(1999\)](#) resulted in the  
237 best correlation between the model-predicted temperatures and data used for  
238 comparison. Sea surface temperatures at locations  $E_1$  and  $E_2$  were obtained from the  
239 NOAA-CIRES CDC analysis/forecast system, whereas surface and nearbed  
240 temperatures at location  $E_3$  were measured in-situ (Horsburgh, 1999); for locations  
241 of  $E_1 - E_3$  see Figure 4(a).

242 The model revealed particularly good capabilities to simulate proper values of  
243 temperatures in the western Irish Sea region ( $E_3$ ) as presented in Figure 4(c), with  $R^2$   
244 values of 95.6% and 96.0% for surface and nearbed temperatures, respectively (see  
245 also Dabrowski et al. (2010) for more details). With regards to locations  $E_1$  and  $E_2$ ,  
246 the  $R^2$  values averaged at 93.4% and 87.2%, respectively. The validation of the  
247 model results against temperature in a stratified region of the Irish Sea is particularly  
248 important due to the influence of thermal fronts on water circulation in the region.

249 Two other heat flux bulk formulae were tested as part of this study resulting in  
250 slightly worse predictions when compared to data; for detailed intercomparison of  
251 the performance of various heat flux models see Dabrowski (2005).

252 In the western Irish Sea cold relict water is preserved in a dome-like shape  
253 throughout summer, as shown in Figure 4(b). The location of transect is shown in  
254 Figure 4(a). Strong thermocline and horizontal thermal fronts are clearly visible; the  
255 upper boundary of the dome is located approximately at 20 m depth below surface.  
256 This temperature structure strictly corresponds to density structure; this result is  
257 consistent with observations reporting the presence of colder, denser water lying  
258 below 20 – 40 m water depth (Hill et al., 1997).

259 Since the dome is static, the sloping density surfaces bounding it can only be  
260 maintained in geostrophic balance by cyclonic surface layer flow (Hill et al., 1997).  
261 Recorded flows are typically between 5-10 cm/s and locally exceed 10 cm/s, and are  
262 approximately front-parallel (Horsburgh et al., 2000). Figure 5(a) presents the  
263 residual circulation reproduced by the model for mid-summer, when stratification is  
264 well developed. As can be seen in Figure 5(a) the model successfully reproduces this  
265 anticlockwise seasonal circulation and the magnitudes of the predicted baroclinic  
266 currents are similar to those reported in Horsburgh et al. (2000). As can also be seen  
267 in Figure 5(b), the barotropic only model does not predict such circulation in the  
268 western Irish Sea region.

269 The reader is referred to Dabrowski (2005), Dabrowski et al. (2010), Olbert et al.  
270 (2010a), Olbert et al. (2010b) and Olbert et al. (2011) for further details on the  
271 model validation including validation of the advection-diffusion model (Olbert et al.,  
272 2010b).

273  
274

## 275 **4. Results and discussion of flushing analysis**

276 Net flows through the Irish Sea have been discussed in [Dabrowski et al. \(2010\)](#) and  
277 in more details in Dabrowski (2005). In this paper we concentrate on the  
278 calculations of residence times and quantification of their spatial variabilities.

279

### 280 **4.1. Residence times**

281 The average residence times obtained for simulations F1-F5 carried out for regions  
282 A-D are summarized in Table 1.

283 The results from the passive tracer transport simulations reveal a significant  
284 variability in the values of the average residence time depending on the forcing

285 functions applied. Both baroclinic and wind induced currents proved to be largely  
286 responsible for increased retention of water within the Irish Sea. The average  
287 residence time of region A obtained in run F4 is greater by as much as 37% when  
288 compared to the tidally only forced model (F1) and equals 386 days; thermohaline  
289 circulation alone increases  $\tau_r$  of region A by 24%, see Table 1 run F3. This shows  
290 the retentive character of baroclinic circulation developing in the Irish Sea. Further  
291 contribution towards increased retention of water in the Irish Sea is due to wind  
292 driven circulation. Similar percentage increases apply also to regions B and C.  
293 Region D, in turn, does not exhibit any significant variability in flushing rates, and,  
294 as can be seen in Table 1, baroclinic circulation does not affect the residence time of  
295 the region (run F3), whereas wind-induced circulation tends to reduce the residence  
296 time only slightly. Region D is shallower than the remaining regions of the Irish Sea,  
297 does not stratify in summer, and is located away from the main channel running  
298 south-north through the Irish Sea, as indicated in Figure 1. Flushing of region D as  
299 well as travel times from the Sellafield's nuclear power plant outfall site located  
300 within this region to various parts of the Irish Sea have been the subject of separate  
301 research presented in Dabrowski and Hartnett (2008).

302 Also, as shown in Table 1, water contained within regions A-C on the 1st of  
303 December, will have a greater residence time by about two months than that  
304 contained there on the 1<sup>st</sup> of June. This is not surprising when the annual variation in  
305 net flows through the Irish Sea is considered. Dabrowski et al. (2010) conclude that  
306 the material contained within the Irish Sea in December will be initially transported  
307 northward at high rates; however it will be returned to the regions over the next three  
308 months as the flow reverses southward. In contrast, for the summer release the  
309 northward transport is predicted for the first three months; the rates are significantly  
310 lower when compared to those in December. It is followed by c.1.5 months of

311 southward transport, however the rates are low. The flow then reverses to northward  
312 and the magnitude progresses quickly to high values in December. The above  
313 pattern results in higher values of the residence time of water in regions A-C in the  
314 case of winter release (F5) when compared to the summer release (F4). Since region  
315 D is located beyond the main channel, it is not subject to the above variability and  
316 thus the summer and winter residence times are virtually identical.

317 Previous estimates of residence times in the Irish Sea include those by Jefferies et al.  
318 (1982), who used observed distributions of  $^{137}\text{Cs}$  and obtained the value 530 days for  
319 region B. He also considered region D separately and calculated the residence time  
320 of 290 days for this region. Further studies, carried out by McKay and Baxter (1985)  
321 and McKay and Pattenden (1993), delivered significantly lower residence times of  
322 region B of approximately 360 days. Values obtained by the authors of this research  
323 are closer to the latter estimate and equal 263 and 338 days, for the summer and  
324 winter tracer releases, respectively. Due to high spatial resolution in which transport  
325 processes have been addressed in this study, the authors believe the proposed  
326 estimates are more reliable.

327

#### 328 **4.2. Spatial distribution of residence time and flushing homogeneity curves**

329 Spatial distributions of residence times in the domain, obtained using the  
330 methodology described in Section 2.2, are presented in Figure 6. Fully forced  
331 models were considered, therefore Figure 6 presents the results obtained from runs  
332 F4 (summer release) and run F5 (winter release) in regions A-D. As far as the entire  
333 region of the Irish Sea is concerned (region A), the St. George's Channel is flushed  
334 initially due to predominant northward flow in the case of both summer and winter  
335 tracer releases, and backwater is formed in the eastern Irish Sea with the maximum  
336 residence times predicted in the coastal waters near Liverpool. However, some

337 significant differences in flushing pathways between runs F4 and F5 are also  
338 predicted. Waters adjacent to the Irish coast from c.50 km south of Dublin  
339 northward are renewed considerably quicker in the event of the winter release (F5).  
340 Tracer concentration in these waters drops below the  $e$ -fold value after about a year  
341 following its introduction. Hence, it coincides with the predicted strong northward  
342 drift, which is most likely responsible for faster tracer removal in this area. In the  
343 case of the summer release, after the time period of 7 months southward flow is  
344 predicted (see Dabrowski et al. (2010)), and also after one year the gyre in the  
345 western Irish Sea is developed. Therefore, water is retained in the area from c.50km  
346 south of Dublin northward for a longer time. Other differences in predicted  
347 residence times include locations near the Welsh coast in the St.George's Channel,  
348 where higher values are predicted in the case of the winter tracer release. The  
349 analysis of region B show that its western part is flushed significantly faster in both  
350 F4 and F5 runs. The areas characterised by the greatest values of residence times are  
351 in the south-east of the region, where backwater is formed. It can also be seen that  
352 the western part of region B is flushed faster in the case of summer release when  
353 compared to the winter release, due to a strong northward drift developing in the  
354 Irish Sea in autumn (see Dabrowski et al. (2010)). High variability in flushing of  
355 region C between the two runs is also apparent. Particularly interesting is also the  
356 strong gradient of the residence time values between the southern and northern parts  
357 of the region predicted by the model in run F5, including the Irish coastal areas As  
358 far as region D is concerned, areas surrounding the Isle of Man are well flushed, and  
359 introduced material stays for longer time mostly within south-east of the region in  
360 the case of both summer and winter releases. In contrast to other regions, similarity  
361 in the distribution of the residence time between the two runs is apparent. Only

362 slightly increased retention in case of the summer release can be noted. This fact is  
363 also reflected in the values of the average residence times given in Table 1.

364 Flushing homogeneity curves for the examined region for the runs F4 and F5 are  
365 presented in Figure 7. In general, the steeper the flushing homogeneity curve the less  
366 variation in the values of residence times throughout the examined region. A  
367 hypothetical completely mixed basin would yield vertical flushing homogeneity  
368 curve. Figure 7 also confirms that there are significant differences in the spatial  
369 distribution of residence time depending on the time of the tracer release.

370 As can be seen in Figure 7, 60% of region A has the values of residence time greater  
371 than 500 days in the case of the summer release of tracer. Considering the winter  
372 release, this value drops to around 35%. On the other hand, c.150 days are required  
373 to renew water in the 10% of the area in the case of the summer release, whereas in  
374 the case of the winter release this time doubles. Similarly for regions B and C, it can  
375 be seen that the time required to flush the initial 10% of the area is significantly  
376 higher in the case of the winter release. Since gradients of the curves following the  
377 initial flushing of c.10% of the areas are similar, therefore it is concluded that this  
378 initial time is the major contributor towards increased average residence times in the  
379 case of winter releases. It can also be noted that region D differs in this regard: the  
380 time required to flush the initial 10% of the area is slightly lower in the case of  
381 winter release. Also, the curves are of similar shape and therefore the average  
382 residence times of the region are virtually the same, as presented in Table 1. The  
383 characteristic shapes of the curves indicate that although large parts of the regions  
384 are characterised by similar values of residence times, there are also places where  
385 sharp gradients in  $\tau_e$  can be expected. This is represented by a characteristic 'step'  
386 on the FHC; the most pronounced being on the FHC for region A and summer  
387 release of tracer (see Figure 7(a)). Figure 7(a) shows that only a small percentage of



388 the area features  $\tau_e$  between c.300 and c.500 days, and for  $\tau_e$  of more than 500 days  
389 the gradient of the curve is significantly greater. This characteristic ‘step’ indicates  
390 that the domain is divided into slow and fast flushing systems, in relative terms and  
391 that high gradient in the values of  $\tau_e$  exist in the transition zone. This phenomenon  
392 can be noted in Figure 6, and is particularly apparent in the case of summer release  
393 in region A, where a sharp gradient is observed in the northern part of the St.  
394 George’s Channel. It is worth noting that this divides energetic waters of the above  
395 channel from relatively slack waters of the Western Irish Sea.

396 Table 2 summarizes FDI for each FHC presented in Figure 7. The higher the value  
397 of the index the shallower the gradient of the curve and the greater the aerial  
398 deviation from mean. The highest value of FDI of 470 days is observed for region A  
399 and summer release (run F4), which is mainly due to the presence of sharp transition  
400 zone from quickly to slowly flushed regions, reflected by a characteristic step on the  
401 curve. FDI is significantly lower in the case of winter release indicating significant  
402 temporal difference in flushing pathways in the region. FDI values for other regions  
403 are lower (steeper curves) and less significant difference is observed for the two  
404 tracer releases considered. Region C is characterised by the lowest values of FDI  
405 and their summer and winter values are virtually the same, indicating similar  
406 average slope of FHC. Interestingly, as presented in Table 1,  $\tau_r$  of this region in the  
407 case of winter tracer release is c.20% greater than in the case of summer release. It  
408 can be therefore concluded that this notable increase in the value of  $\tau_r$  is attributed to  
409 the significant increase in the residence times of the quickest flushed areas. Indeed,  
410 as can be seen in Figure 7,  $\tau_{e10\%}$  for this region increases from 105 days in the case  
411 of summer release to 160 days in the case of winter release.

412  
413

414 **5 Summary and Conclusions**

415 This paper presents details of research into developing a better understanding of the  
416 assimilative capacity of the Irish Sea; a novel generic approach for flushing studies  
417 has been proposed as part of this research. With regards to the Irish Sea modelling,  
418 particular emphasis was put on the proper representation of thermal stratification  
419 developing in the western Irish Sea during spring and summer. Flushing  
420 characteristics considered include average residence time, spatially distributed  
421 residence times, flushing homogeneity curve and flushing deviation index.

422 The main conclusions resulting from this research are summarized and discussed  
423 below:

- 424 • This research illustrates that the proposed new approach using spatial  
425 distribution of residence times and flushing homogeneity curves gives new  
426 insight into flushing of the Irish Sea and transport processes. Since the Irish  
427 Sea is a hydrographically complex system, a single value describing its  
428 flushing properties delivers a picture that is incomplete. It has been shown  
429 that even within hydrographically uniform subregions, further valuable  
430 information is obtained through the adaptation of the proposed approach,  
431 namely the compact visualisation of flushing pathways and quantification of  
432 the variation in flushing.
- 433 • The authors showed that not only the average residence times of various  
434 regions of the Irish Sea vary depending on the time of the year selected as  
435 the start date for the examination of the water renewal processes, but spatial  
436 distributions of residence times within these regions also differ. For example,  
437 sharp gradients in the values of residence times are predicted in the case of  
438 winter release that separate relatively quickly flushed St. George's Channel  
439 from the remaining relatively slowly flushed regions; the gradient is

440 significantly lower in the case of the summer release. Discrepancies within  
441 the St. George's Channel are also apparent when the region is considered  
442 separately. Relatively small variation in flushing pathways between summer  
443 and winter releases is observed in the eastern Irish Sea; this is consistent with  
444 the results on average residence times, which reveal region's stable flushing  
445 properties. Thus, plotting the distributed residence times for a region gives a  
446 second-order insight into the transport phenomena, and is therefore a useful  
447 complement to flow fields provided by the hydrodynamic model along with  
448 the general information provided by single values of average residence times.

- 449 • The concept of FHC was devised by the authors and then applied to  
450 summarize flushing properties. FHCs provide useful generic information  
451 about the degree of variation in flushing rates across the domain. In  
452 particular, the range of the values of residence time is delivered as well as the  
453 'smoothness' of transition from quickly to slowly flushed regions. For  
454 example, curves of shallow gradients indicate higher spatial variability in  
455 residence times. Also, points of contraflexure and characteristic 'step' on the  
456 curve indicate the presence of sharp gradients in flushing rates when moving  
457 across the examined region, thus imposing careful management approach.  
458 The average slope of the curve is quantified by FDI. Apart from bringing in  
459 some more valuable information on the deviation in the values of residence  
460 time from mean, further important conclusions in relation to slowest and  
461 quickest flushed regions can be drawn when analysed in conjunction with  $\tau_r$ .  
462 For example, an increase of  $\tau_r$  without change of FDI indicates an increase in  
463 residence times of the quickest flushed regions. Therefore, FHC, FDI and  $\tau_r$   
464 may be utilised in determining the need of more detailed studies of transport  
465 and water renewal studies prior to making important management decisions.

466 • This research showed that average residence times of the Irish Sea and its  
467 subregions are functions of tidal action, meteorological conditions and  
468 density-driven currents, and thus also the time of the year considered. As far  
469 as the entire region of the Irish Sea and summer tracer release are concerned,  
470 tidal circulation alone flushes the domain in 282 days. When wind induced  
471 flows are included, the average residence time increases to 322 days. Finally,  
472 the average residence time of 386 days is computed when thermohaline  
473 circulation is also included; this is 37% increase when compared to tidal  
474 model. Regions B and C that were considered separately exhibit similar  
475 response to various forcing functions applied. In the case of a winter tracer  
476 release, further 15-28% increase in the values of average residence times is  
477 observed, depending on the region. In contrast, the eastern Irish Sea (region  
478 D) is characterised by relatively stable residence times. This significant  
479 variation in flushing properties was then investigated in more details using  
480 the new approach devised in this research. This is an extremely useful  
481 approach considering significant implications for management of water  
482 quality, particularly with regards to the discharge of persistent pollutants,  
483 such as radionuclides.

484

#### 485 **Acknowledgements**

486 The authors wish to acknowledge the Environmental Protection Agency, Ireland, for  
487 funding this research project.

488 NCEP Reanalysis data provided by the NOAA-CIRES Climate Diagnostics Center,  
489 Boulder, Colorado, USA, from their Web site at <http://www.cdc.noaa.gov/>.

490 UK Tide Gauge data and water currents records provided by the British

491 Oceanographic Data Centre, from their website at <http://www.bodc.ac.uk>.

492

493

494

### References

- 495 [Ahsan, A.K.M.Q., Blumberg A.F., 1999. Three-Dimensional Hydrothermal Model](#)  
496 [of Onondaga Lake, New York. Journal of Hydraulic Engineering 125\(9\), 912-923.](#)
- 497 [Asselin, S., Spaulding, M.L., 1993. Flushing times for the Providence River based](#)  
498 [on tracer experiments. Estuaries 16\(4\) 830-839.](#)
- 499 [Blumberg, A.F., Mellor, G.L., 1987. A description of a three-dimensional coastal](#)  
500 [ocean circulation model. In Three-Dimensional Coastal Ocean Models, ed. N.](#)  
501 [Heaps. American Geophysical Union, Washington, D.C., pp. 1-16.](#)
- 502 [Bolin, B., Rodhe, H., 1973. A note on the concepts of age distribution and transit](#)  
503 [time in natural reservoirs. Tellus 25\(1\), 58-62.](#)
- 504 [Bowden, K.F., 1980. Physical and dynamical oceanography of the Irish Sea. In:](#)  
505 [Banner, F.T., Collins, W.B., Massie, K.S. \(Eds.\), The north-west European shelf](#)  
506 [seas: the seabed and the sea in motion. II Physical and chemical oceanography and](#)  
507 [physical resources. Elsevier, Amsterdam, Oxford and New York, pp. 391-413.](#)  
508
- 509 [Cohen, J.E., Small, C., Mellinger, A., Gallup, J., Sachs, J., Vitousek, P.M., Mooney,](#)  
510 [H.A., 1997. Estimates of coastal populations. Science 278, 1211-1212.](#)  
511
- 512 [Dabrowski, T., 2005. A flushing study analysis of selected Irish waterbodies. Ph.D.](#)  
513 [Thesis, Civil Engineering Department, National University of Ireland, Galway,](#)  
514 [411pp.](#)  
515
- 516 [Dabrowski, T., Hartnett, M., 2008. Modelling travel and residence times in the](#)  
517 [eastern Irish Sea. Marine Pollution Bulletin 57, 41-46.](#)  
518
- 519 [Dabrowski, T., Hartnett, M., Olbert, A.I., 2010. Influence of seasonal circulation on](#)  
520 [flushing of the Irish Sea. Marine Pollution Bulletin 60\(5\), 748-58.](#)  
521
- 522 [Dyer, K.R., 1997. Estuaries: a physical introduction. John Wiley and Sons Ltd.,](#)  
523 [London, 210pp.](#)  
524
- 525 [Hill, A.E., Brown, J., Fernand, L., 1996. The western Irish Sea gyre: a retention](#)  
526 [system for Norway Lobster \(\*Nephrops norvegicus\*\). Oceanologica Acta 19, 357-368.](#)  
527
- 528 [Hill, A.E., Brown, J., Fernand, L., 1997. The summer gyre in the western Irish Sea:](#)  
529 [Shelf sea paradigms and management implications. Estuarine, Coastal and Shelf](#)  
530 [Science 44, 83-95.](#)  
531
- 532 [Horsburgh, K.J., 1999. Observations and modelling of the Western Irish Sea Gyre.](#)  
533 [Ph.D. Thesis, School of Ocean Sciences, Bangor, United Kingdom, University of](#)  
534 [Wales, Bangor, 171pp.](#)  
535

536 [Horsburgh, K.J., Hill, A.E., Brown, J., Fernand, L., Garvine, R.W., Angelico,](#)  
537 [M.M.P., 2000. Seasonal evolution of the cold pool gyre in the western Irish Sea.](#)  
538 [Progress in Oceanography, 46\(1\), 1-58.](#)

539 HydroQual Inc., 2002. A Primer for ECOMSED, Version 1.3. Users Manual.  
540 HydroQual, Mahwah, NJ, 188pp.  
541

542 ISSG, 1991. The Irish Sea: An environmental review. Part 2: Waste inputs and  
543 pollution. Irish Sea Study Group Report. Liverpool University Press, Liverpool.  
544

545 [Jefferies, D.F., Steele, A.K., Preston, A., 1982. Further studies on the distribution of](#)  
546 [<sup>137</sup>Cs in British coastal waters - I. Irish Sea. Deep-Sea Research 29\(6A\), 713-738.](#)

547 [Luketina, D., 1998. Simple tidal prism models revisited. Estuarine, Coastal and](#)  
548 [Shelf Science 46, 77-84.](#)  
549

550 [McKay, W.A., Baxter, M.S., 1985. Water transport from the North-east Irish Sea to](#)  
551 [western Scottish coastal waters: Further observations from time-trend matching of](#)  
552 [Sellafield radiocaesium. Estuarine, Coastal and Shelf Science 21, 471-480.](#)

553 McKay, W.A., Pattenden, N.J., 1993. The behaviour of Plutonium and Americium in  
554 the shoreline waters of the Irish Sea: A review of Harwell Studies in the 1980s.  
555 Journal of Environmental Radioactivity 18, 99-132.  
556

557 [Mellor, G.L., Yamada, T., 1982. Development of a turbulence closure model for](#)  
558 [geophysical fluid problems. Rev. Geophys. Space Phys. 20, 851-875.](#)

559 [Mellor, G.L., 2001. One-dimensional, ocean surface modeling, a problem and a](#)  
560 [solution. Journal of Physical Oceanography 31, 790-809.](#)

561 [Mellor, G.L., 2003. Users guide for a three-dimensional, primitive equation,](#)  
562 [numerical ocean model. In, Program in Atmospheric and Oceanic Sciences,](#)  
563 [Princeton University, Princeton, NJ.](#)

564 Meteorological Service, 1995. Monthly Weather Bulletin. Meteorological Service,  
565 Glasnevin Hill, Dublin 9.  
566

567 [Murakami K., 1991. Tidal exchange mechanism in enclosed regions. Proceedings of](#)  
568 [the 2nd International Conference on Hydraulic Modelling of Coastal Estuaries and](#)  
569 [River Waters, pp. 111-120.](#)  
570

571 [Olbert, A.I., Hartnett, M., Dabrowski, T., 2010a. Assessment of Tc-99 monitoring](#)  
572 [within the western Irish Sea using a numerical model. Science of the Total](#)  
573 [Environment 408, 3671-3682.](#)  
574

575 [Olbert, A.I., Hartnett M., Dabrowski, T., Kelleher, K., 2010b. Effects of complex](#)  
576 [hydrodynamic processes on the horizontal and vertical distribution of Tc-99 in the](#)  
577 [Irish Sea. Science of the Total Environment 409, 150-161.](#)  
578

579 [Olbert, A.I., Hartnett, M., Dabrowski, T., Mikolajewicz, U., 2011. Long-term inter-](#)  
580 [annual variability of a cyclonic gyre in the western Irish Sea. Continental Shelf](#)  
581 [Research 31, 1343-1356.](#)

582  
583 [Prandle, D., 1984. A modelling study of the mixing of 137Cs in the seas of the](#)  
584 [European continental shelf. Philosophical Transactions of the Royal Society of](#)  
585 [London 310, 407-436.](#)  
586  
587 Proctor, R., 1981. Tides and residual circulation in the Irish Sea. Ph.D. Thesis,  
588 Univeristy of Liverpool, Liverpool, UK.

589 [Ramster, J.W., Hill, H.W., 1969. Currents systems in the northern Irish Sea. Nature](#)  
590 [244, 59-61.](#)  
591  
592 [Simpson, J.H., Hunter, J.R., 1974. Fronts in the Irish Sea. Nature 250, 404-406.](#)  
593  
594 [Simpson, J.H., Hughes, D.G., Morris, N.C.G., 1977. The relation of seasonal](#)  
595 [stratification to tidal mixing on the continental shelf. In: Angel, M., \(ed.\), A Voyage of](#)  
596 [Discovery, Supplement to Deep-Sea Research, George Deacon 70<sup>th</sup> Anniversary](#)  
597 [Volume, pp. 327-340. Pergamon Press.](#)

598 [Smagorinsky, J., 1963. General circulation experiments with the primitive equations,](#)  
599 [I. The basic experiment. Monthly Weather Review 91, 99-164.](#)

600 [Smolarkiewicz, P., 1984. A fully multidimensional positive definite advection](#)  
601 [transport algorithm with small implicit diffusion. Journal of Computational Physics](#)  
602 [54, 325-362.](#)

603 [Takeoka, H., 1984. Fundamental concepts of exchange and transport time scales in a](#)  
604 [coastal sea. Continental Shelf Research 3\(3\), 311-326.](#)

605 [van de Kreeke, J., 1983. Residence time: Application to small boat basins. Journal of](#)  
606 [Waterway, Port, Coastal, and Ocean Engineering 109\(4\), 416-428.](#)

607 [Wang, S., McGrath, R., Hanafin, J., Lynch, P., Semmler, T., Nolan, P., 2008. The](#)  
608 [impact of climate change on storm surges over Irish waters. Ocean Modelling 25,](#)  
609 [83-94.](#)  
610  
611 Zimmerman, J.T.F., 1976. Mixing and flushing of tidal embayments in the western  
612 Dutch Wadden Sea: Part I. Distribution of salinity and calculation of mixing time  
613 scales. Netherland Journal of Sea Research 10(2), 149-191.  
614  
615  
616  
617  
618  
619 List of Figures:  
620  
621 **Figure 1.** The Irish Sea bathymetry and model orientation. Contours of 80 m water depth are  
622 highlighted to show the extents of the main channel. Distribution of the field data  
623 collected for the model set-up and calibration is also presented.  
624  
625 **Figure 2.** Extents of the region of the Irish Sea selected for flushing studies.

626 **Figure 3.** Barotropic model validation: (a) maximum depth averaged tidal currents  
 627 during an average spring tide, (b) distribution of tidal mixing ratio  
 628 predicted by the model (see [Simpson et al. \(1977\)](#) for comparison), (c)  
 629 comparison of modelled and recorded tidal elevations at T4 over a spring-  
 630 neap tidal cycle and (d) measured and modelled current speeds at B3 over  
 631 a tidal cycle.  
 632

633 **Figure 4.** (a) Location of a transect and temperature stations E1-E3, (b) transverse  
 634 section through the western Irish Sea showing modelled temperatures and  
 635 (c) comparison of modelled and recorded temperatures at station E3.  
 636

637 **Figure 5.** Residual circulation in the surface layer predicted by (a) barotropic and baroclinic  
 638 model and (b) tidal model. Presented area is delineated in Figure 1. The extent of  
 639 the western Irish Sea gyre is shown.  
 640

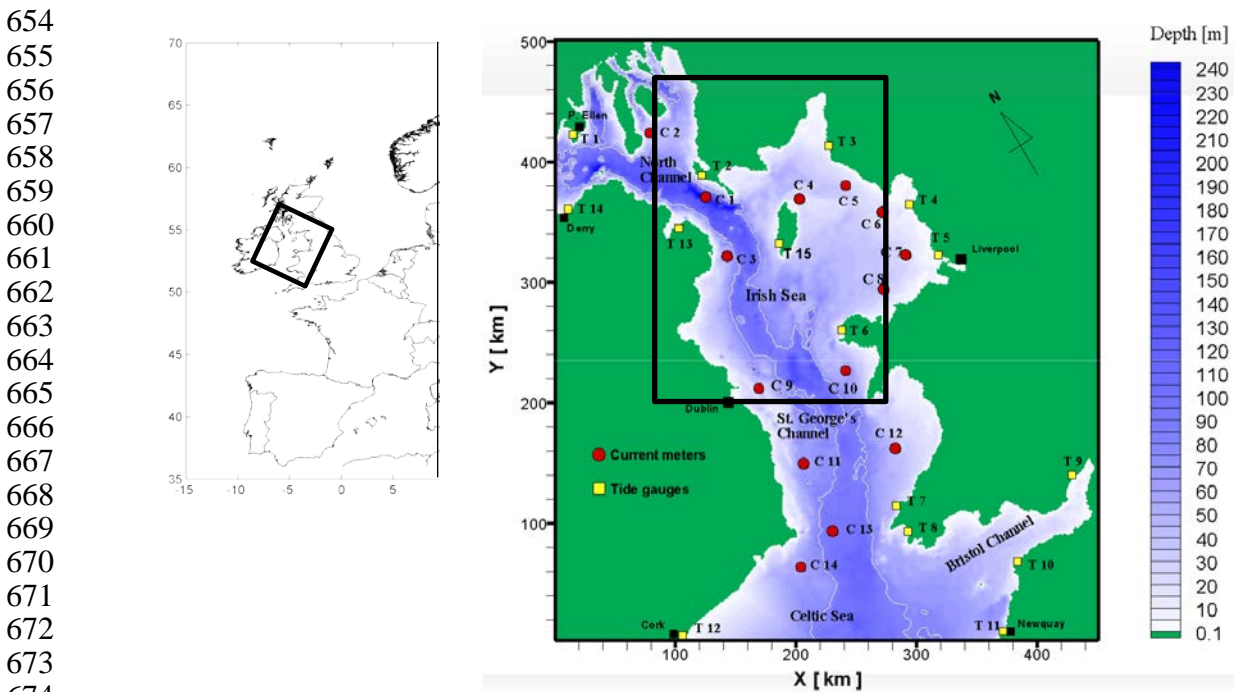
641 **Figure 6.** Spatial distributions of residence times in regions A-D of the Irish Sea calculated  
 642 from runs F4 and F5 of the model.  
 643

644 **Figure 7.** Flushing homogeneity curves of regions A-D of the Irish Sea obtained from  
 645 model runs (a) F4 and (b) F5.  
 646

647  
 648  
 649 **List of Tables:**

650  
 651 **Table 1.** Characterisation of model runs and values of calculated residence times.  
 652

653 **Table 2.** Values of FDI for regions A-D and model runs F4 and F5.  
 654



675 **Figure 1.** The Irish Sea bathymetry and model orientation. Contours of 80 m water depth are  
 676 highlighted to show the extents of the main channel. Distribution of the field data  
 677 collected for the model set-up and calibration is also presented.  
 678  
 679



680  
681  
682  
683  
684  
685  
686  
687  
688  
689  
690  
691  
692  
693  
694  
695  
696  
697  
698  
699  
700  
701  
702  
703  
704  
705  
706  
707  
708  
709  
710  
711  
712  
713  
714  
715  
716

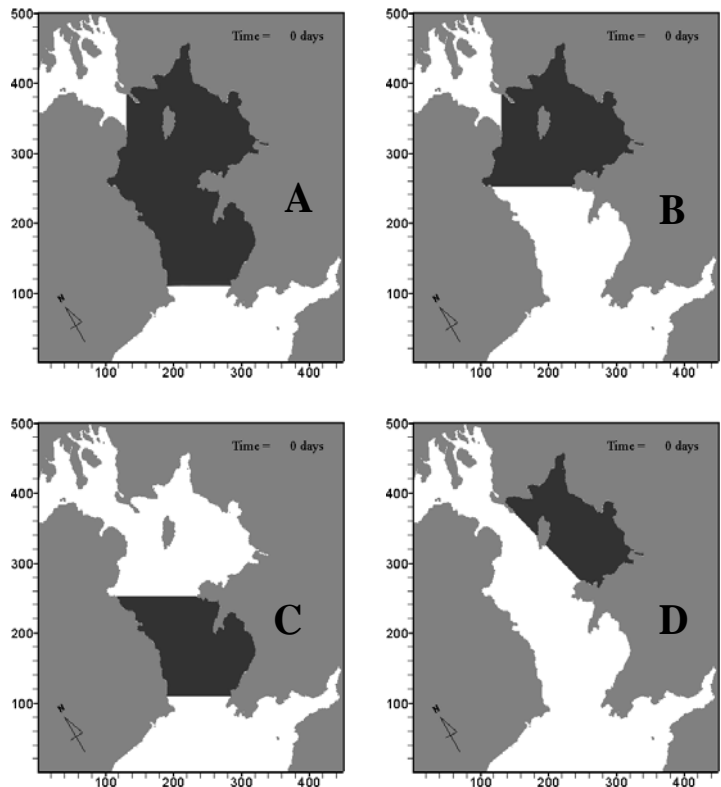
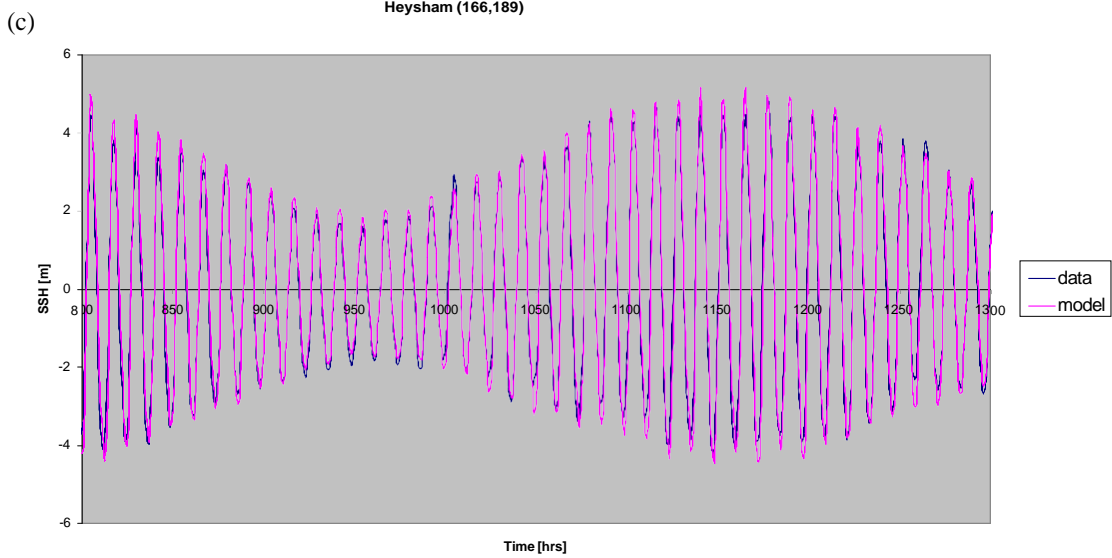
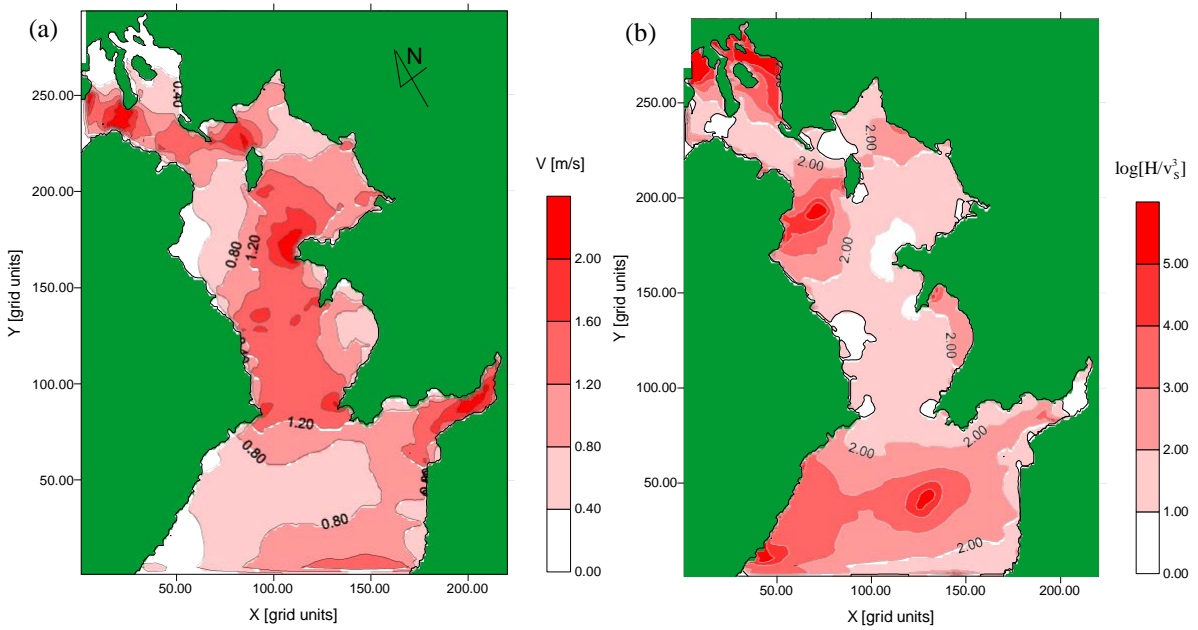


**Figure 2.** Extents of the regions of the Irish Sea selected for flushing studies.

717  
718  
719  
720  
721  
722  
723  
724  
725  
726  
727  
728  
729

730  
731  
732  
733  
734  
735  
736  
737  
738  
739  
740  
741  
742  
743  
744  
745  
746



747  
748  
749  
750  
751  
752  
753  
754  
755  
756  
757  
758  
759  
760  
761  
762  
763  
764  
765  
766

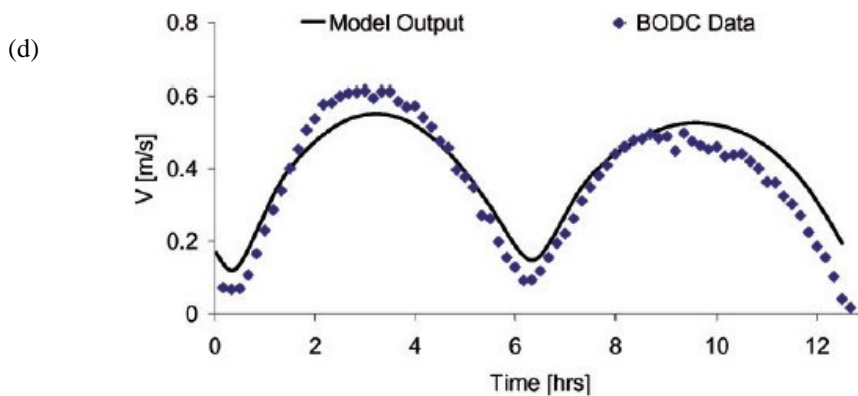


**Figure 3.** Barotropic model validation: (a) maximum depth averaged tidal currents during an average spring tide, (b) distribution of tidal mixing ratio predicted by the model (see Simpson et al. (1977) for comparison), (c) comparison of modelled and recorded tidal elevations at T4 over a spring-neap tidal cycle and (d) measured and modelled current speeds at B3 over a tidal cycle.

767  
768  
769  
770  
771  
772  
773  
774  
775  
776  
777  
778  
779  
780  
781  
782  
783  
784  
785  
786  
787  
788  
789  
790  
791  
792  
793  
794  
795  
796  
797  
798  
799  
800  
801  
802  
803  
804  
805  
806  
807  
808  
809  
810  
811  
812  
813  
814  
815  
816  
817  
818  
819

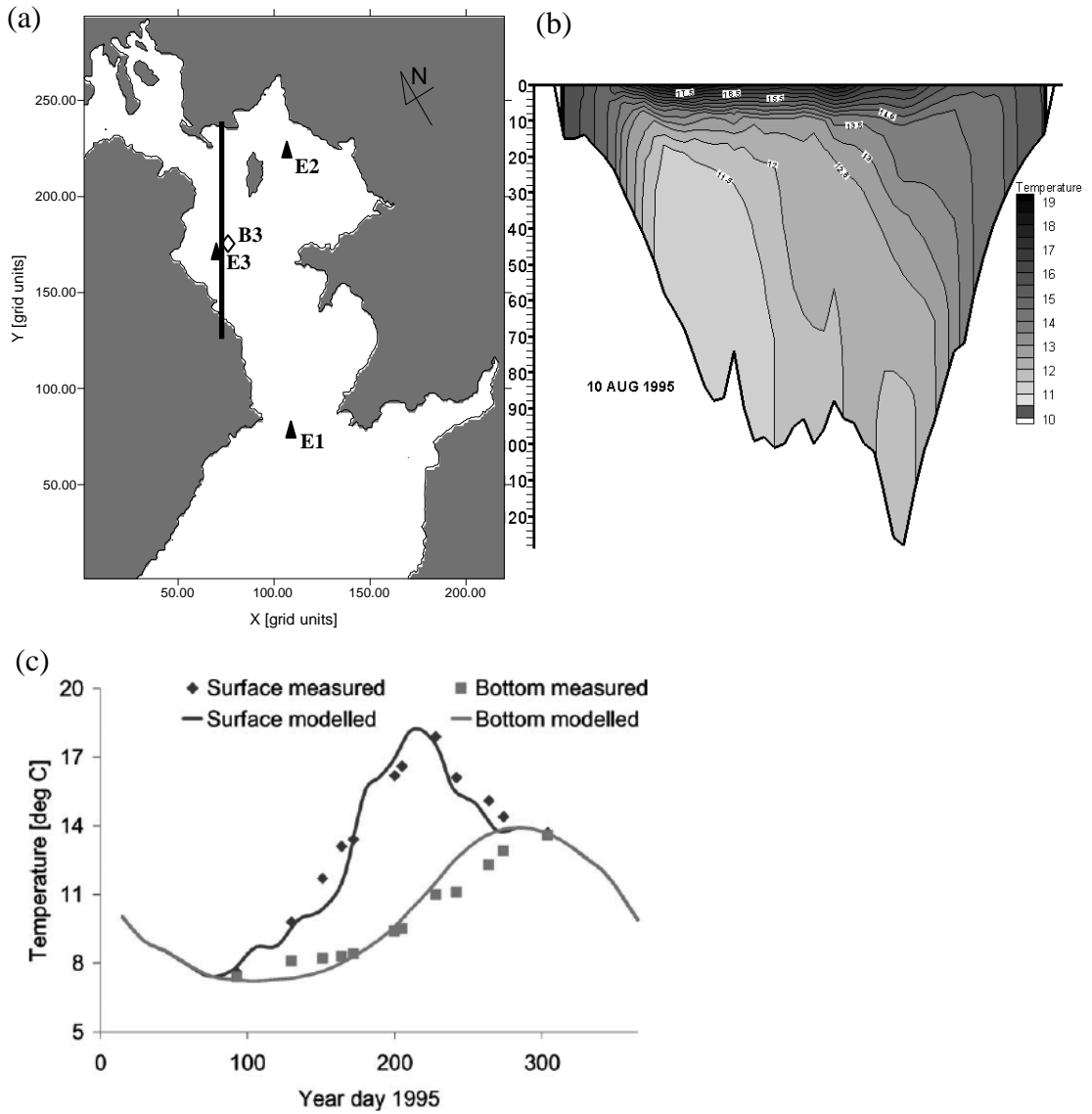


**Figure 4.** (a) Location of a transect and temperature stations E1-E3, (b) transverse section through the western Irish Sea showing modelled temperatures and (c) comparison of modelled and recorded temperatures at station E3.

820  
821  
822  
823  
824  
825  
826  
827  
828  
829  
830  
831  
832  
833  
834  
835  
836  
837  
838  
839  
840  
841  
842  
843  
844  
845  
846  
847  
848  
849  
850  
851  
852  
853  
854  
855  
856  
857  
858  
859  
860  
861  
862  
863  
864  
865  
866  
867  
868  
869  
870  
871

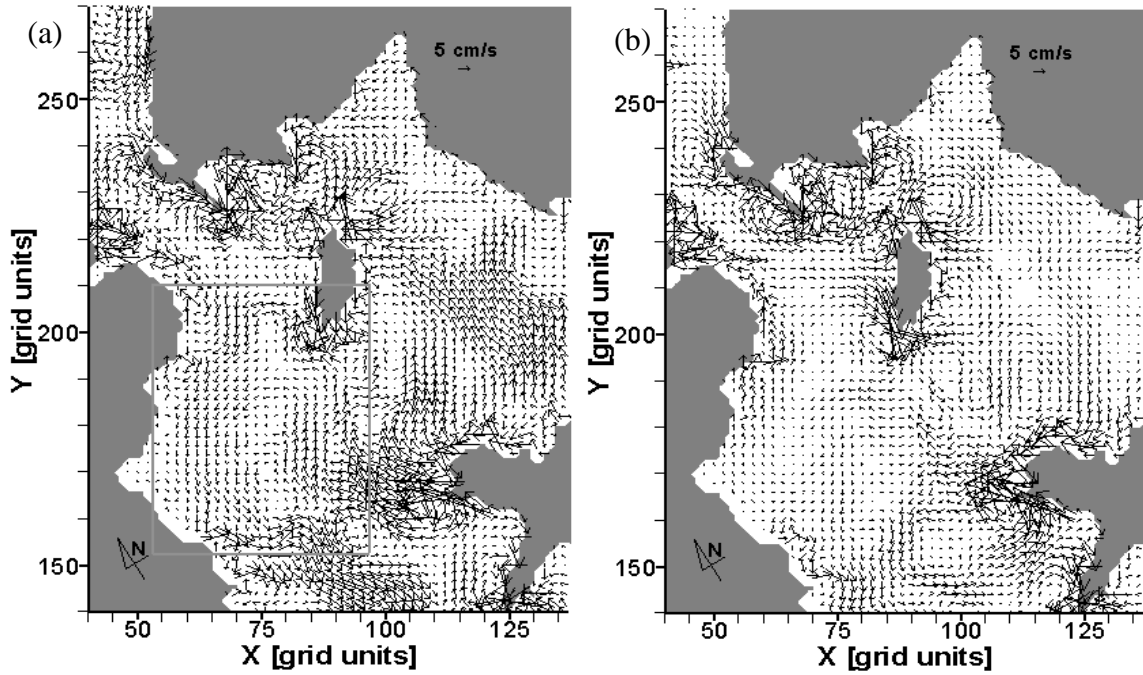


**Figure 5.** Residual circulation in the surface layer predicted by (a) barotropic and baroclinic model and (b) tidal model. Presented area is delineated in Figure 1. The extent of the western Irish Sea gyre is shown.

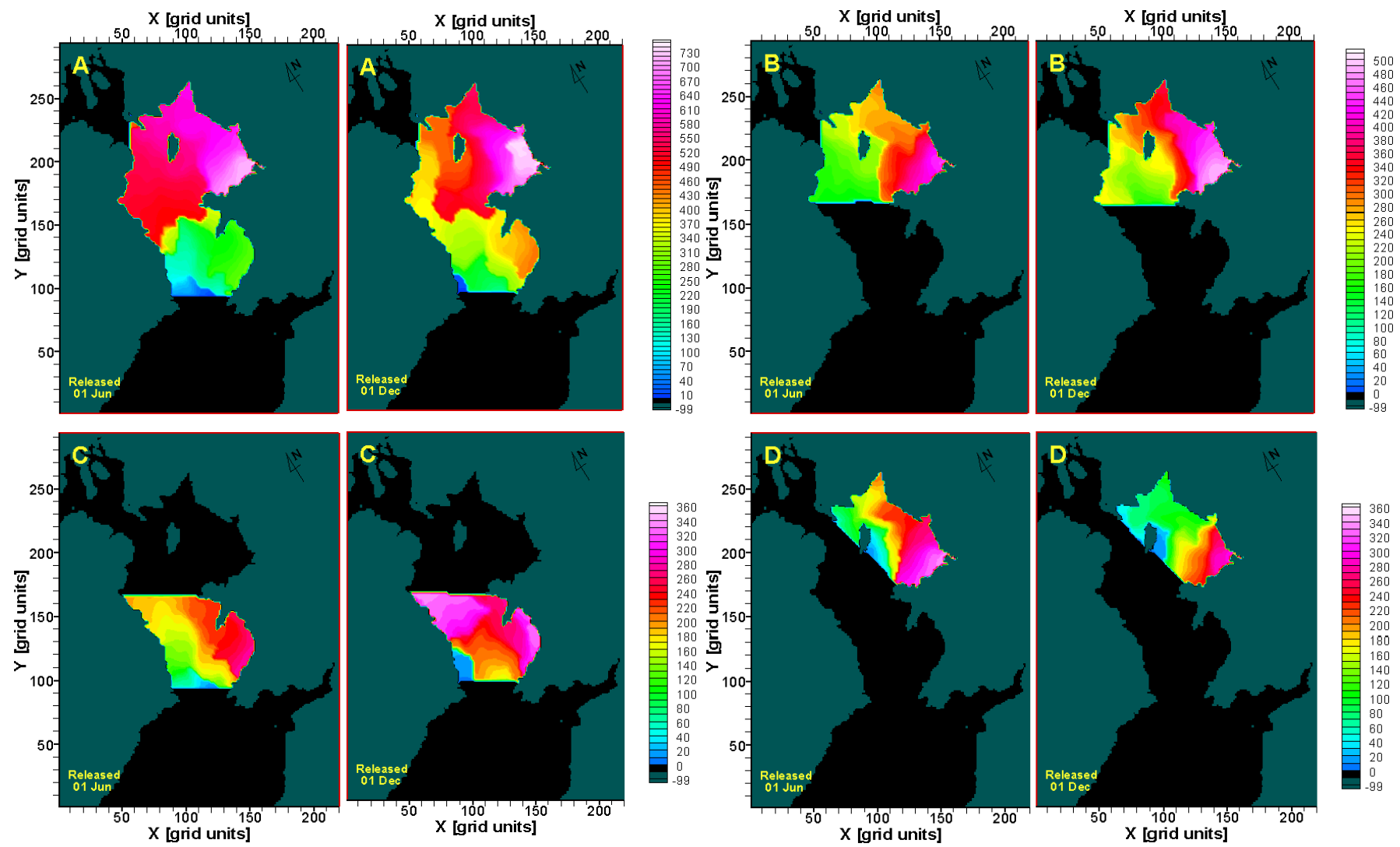
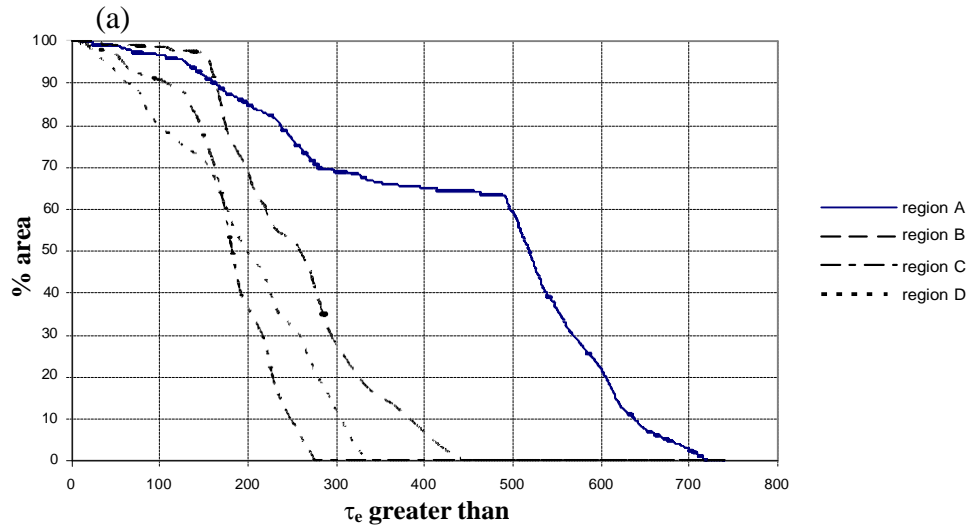
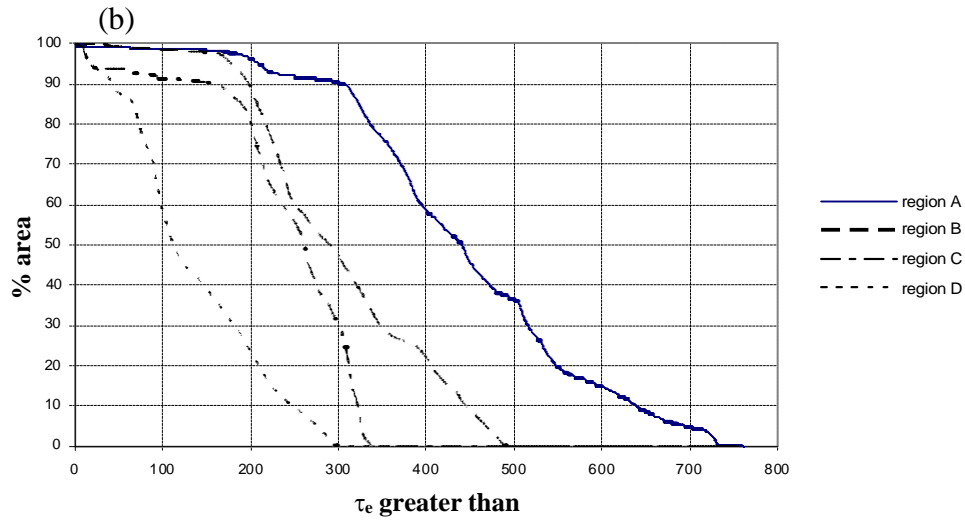


Figure 6. Spatial distributions of residence times in regions A-D of the Irish Sea calculated from runs F4 and F5 of the model.

878  
879



880  
881



882  
883  
884  
885  
886  
887  
888  
889

**Figure 7.** Flushing homogeneity curves of regions A-D of the Irish Sea obtained from model runs (a) F4 and (b) F5.

890 **Table 1.** Characterisation of model runs and values of calculated residence times.

Model run	Run characteristic		Residence times for regions A-D			
	Dye release date	Model version	$\tau_{rA}$ (d)	$\tau_{rB}$ (d)	$\tau_{rC}$ (d)	$\tau_{rD}$ (d)
F1	01 Jun	tides only	282	214	154	224
F2	01 Jun	tides + wind	322	219	179	209
F3	01 Jun	tides + heat flux	351	257	179	223
F4	01 Jun	tides + wind + heat flux	386	263	203	213
F5	01 Dec	tides + wind + heat flux	444	338	244	208

891

892

893 **Table 2.** Values of FDI for regions A-D and model runs F4 and F5.

<b>Model run</b>	<b>FDI<sub>A</sub> (d)</b>	<b>FDI<sub>B</sub> (d)</b>	<b>FDI<sub>C</sub> (d)</b>	<b>FDI<sub>D</sub> (d)</b>
F4	470	215	145	245
F5	330	245	155	205

894

895

896

897

898